A turbulent flame speed closure model for LES of industrial burner flows

By **P. Flohr**† and **H. Pitsch**

A combustion model based on a turbulent flame speed closure (TFC) model is proposed for large-eddy simulations (LES) of lean premixed combustion in industrial gas turbine burners. This model has been originally proposed in a RANS context; the extension to LES is found to be fairly straight-forward, i.e. the turbulent quantities that determine the turbulent flame speed are obtained at the level of the grid cut-off. The model has been applied to a simple premixed jet flame in a backward-facing step combustor to investigate the combustor response to forced excitations.

1. Introduction

The demand for ever decreasing emissions levels of modern gas turbines has led to the development of lean-premixed combustor technology. Here, low emissions can be achieved by perfecting the premixing of the fuel-air mixture and by operating at low flame temperatures, i.e. fuel-lean conditions. The desire to operate gas turbines in low emission mode over the full engine operating range often brings the combustion process dangerously close to lean extinction. As a consequence, the combustion at part-load levels is often accompanied by thermo-acoustic instabilities which may deteriorate the combustion process or even reduce the combustor life. Therefore, there is a strong need for predicting stability limits of industrial combustors.

LES is often seen as a suitable tool for accurately predicting both flame stability and fuel-air mixing (Angelberger *et al.* 1998). Because the largest turbulence scales are explicitly computed in LES and only the smallest, low-energy modes are modeled (where the assumption of local isotropy is expected to hold better than for the largest scales), the prediction of mean flow and mixing is often found to be superior to classical steady RANS models which frequently fail in the highly turbulent, strongly swirling flows that are typically employed in gas turbine burners (Kim *et al.* 1999). On top of that, it intrinsically captures the unsteadiness of extinction and instability processes.

While LES has reached some degree of maturity for non-reacting flows, its application to reacting flows is still being developed, and various modeling approaches have been proposed in the context of premixed combustion, see Veynante & Poinsot (1997), Peters (2000) and references therein. Most of the proposed models have previously been used, or could very similarly be applied, in steady RANS calculations. This is not surprising because the characteristic length- and time-scales where combustion takes place are typically well below the resolved grid scales, and the combustion process has to be modeled entirely at the subgrid level.

In this work we explore the Turbulent Flame speed Closure (TFC) model, which has

† ALSTOM Power Ltd., Segelhof 1, CH-5405 Baden-Daettwil, Switzerland

previously been successfully applied in a RANS context to gas turbine combustion (Zimont *et al.* 1997, Polifke *et al.* 2000). The model is based on solving the one transport equation in addition to the non-reactive case for the reaction progress variable c. Closure is achieved via a source term involving a turbulent flame speed S_T. The turbulent flame speed is obtained from theoretical analysis based on the assumption that combustion is in the "thickened flamelet" regime, which is typical of premixed combustion at gas turbine conditions. The robustness and efficiency of the model (Polifke *et al.* 2000) render it suitable for engineering applications.

The final goal of this work is to perform LES of unstable combustion processes in industrial burner flows. Here, we apply the model to a generic premix burner that has already been extensively studied, both experimentally and numerically (Poinsot *et al.* 1987; Angelberger *et al.* 1998). This configuration showed strong self-excited instabilities at certain operating conditions and provides an example for the investigation of the mechanisms by which the unsteady flow and heat release fields are coupled; the case is also suitable for determining whether the subgrid closure suggested above is suitable to capture such effects.

In addition to the need for an appropriate combustion subgrid closure, the application of a LES tool to industrial configurations must meet two important criteria: first, the tool has to be able to handle complex geometries and secondly, it must be efficient and robust if it is to be used in a design process. It is, therefore, desirable to incorporate LES models in the frame of standard, unstructured, industrial flow solvers. However, it is not yet clear whether such tools which necessarily have to balance robustness against numerical accuracy and solver speed against model flexibility are suitable for engineering-level LES. Therefore, part of this summer research program included performing a basic test of turbulent pipe flow to assess the LES capabilities of an industrial flow solver.

2. Model formulation

2.1. *The filtered c-equation*

The chemical reaction is described using a progress variable c, which is defined as a normalized mass fraction of products such that $c = 0$ in the unburnt mixture and $c = 1$ in the products. Using the Favre-averaged filtering on the transport equation of the progress variable one obtains

$$\frac{\partial \overline{\rho}\tilde{c}}{\partial t} + \nabla \cdot (\overline{\rho}\tilde{\mathbf{u}}\tilde{c}) = \nabla \cdot (\overline{\rho}\kappa \nabla \tilde{c}) + \nabla \mathbf{q} + \overline{\dot{w}_c} \tag{2.1}$$

where $\tilde{c}$ denotes the Favre-averaged progress variable, such that $\overline{\rho}\tilde{c} = \overline{\rho c}$. κ is the molecular diffusivity, $\mathbf{q}$ incorporates the subgrid fluxes, and $\overline{\dot{w}_c}$ is the reactive source term.

Closure for the subgrid flux

$$\mathbf{q} = \tilde{c}\tilde{\mathbf{u}} - \widetilde{c\mathbf{u}} \tag{2.2}$$

is obtained by making the usual gradient-diffusion assumption

$$\mathbf{q} = \kappa_t \nabla \tilde{c} \tag{2.3}$$

where the eddy diffusivity κ_t is obtained from the turbulent viscosity ν_t by making the assumption of the existence of a turbulent Schmidt number,

$$\kappa_t = \nu_t / \mathrm{Sc}_t. \tag{2.4}$$

In this work, we assume the turbulent Schmidt number to be constant, $\mathrm{Sc}_t = 0.7$, and we obtain the turbulent viscosity from the standard Smagorinski model

$$\nu_t = (C_s \Delta)^2 \sqrt{2\overline{S}_{ij}\overline{S}_{ij}}, \tag{2.5}$$

where $C_s = 0.1$ is a model constant, Δ is the filter cut-off scale, and $\overline{S}_{ij}$ is the large-scale strain rate tensor.

The chemical reaction term in (2.1) is modeled by

$$\overline{\dot{w}_c} = \overline{\rho}_u S_t^{\Delta} |\nabla \tilde{c}|, \tag{2.6}$$

where $\overline{\rho}_u$ is the density of the unburnt mixture and S_t^{Δ} is a turbulent flame speed that depends on the physico-chemical characteristics of the combustible mixture and the local turbulence at the subgrid level. Using (2.3) and (2.6) in (2.1) and neglecting molecular diffusion effects, we obtain

$$\frac{\partial \overline{\rho}\tilde{c}}{\partial t} + \nabla \cdot (\overline{\rho}\tilde{\mathbf{u}}\tilde{c}) = \nabla \left(\overline{\rho} \frac{\nu_t}{\mathrm{Sc}_t} \nabla \tilde{c} \right) + \overline{\rho}_u S_t^{\Delta} |\nabla \tilde{c}|. \tag{2.7}$$

Equation (2.7) describes a combustion front that is characterized by a turbulent flame speed which quickly adapts to a local equilibrium value and a flame brush thickness which grows according to turbulent dispersion by the subgrid scales.

It is noted that the assumption of gradient-diffusion transport is not in contradiction with the existence of counter-gradient diffusion, and counter-gradient transport is, in fact, implicitly modeled in the chemical source term (2.6) as shown by Zimont *et al.* (2000).

For very large times, the increase in thickness of the flame brush is compensated by the local flamelet propagation, and the first term on the right-hand side of (2.7) should be incorporated in the reactive source term. However, it can be shown that the time scale required to achieve this equilibrium is much larger than the integral turbulent time scale τ_t (Zimont *et al.* 2000). In industrial combustors the residence time is usually comparable to the turbulent time τ_t, and (2.7) is therefore the appropriate model equation.

2.2. *Zimont's model of the turbulent flame speed*

For a complete closure in (2.7) one has to provide a model for the turbulent flame speed S_t. The models are usually of the form

$$\frac{S_t}{S_l} = 1 + f(\mathrm{Re}, \mathrm{Da}, \mathrm{Pr}), \tag{2.8}$$

where S_l is the laminar flame velocity and f is a functional of the hydrodynamical and physico-chemical parameters, expressed via the Reynolds, Damköhler, and Prandtl numbers,

$$\mathrm{Re} = \frac{u_t l_t}{\nu}, \quad \mathrm{Da} = \frac{\tau_t}{\tau_c}, \quad \mathrm{Pr} = \frac{\nu}{\chi}. \tag{2.9}$$

u_t, l_t and $\tau_t = l_t/u_t$ are the integral turbulent scales, $\tau_c = \chi/S_l^2$ is the chemical time scale, and χ is the thermal conductivity.

Zimont (1979) proposed a model for S_t which is valid in the "thickened flamelet" regime. This regime is characterized by very large Reynolds numbers and moderately large Damköhler numbers such that

$$\mathrm{Re} \gg 1, \quad 1 < \mathrm{Da} < \mathrm{Re}^{1/2}. \tag{2.10}$$

The second inequality indicates that the Damköhler number is large, but not large enough for the combustion to occur in the laminar flamelet regime. In other words, the laminar flame thickness is much smaller than the integral length l_t but significantly larger than the Kolmogorov scale η. Zimont's (1979) analysis for this regime led to the following expression for the turbulent flame speed

$$\frac{S_t}{S_l} \simeq (\mathrm{RePr})^{1/2}\,\mathrm{Da}^{-1/4} \tag{2.11}$$

Without repeating his analysis, which is based only on dimensional arguments and the existence of a turbulent cascade according to Kolmogorov (1941), we state here his two main modeling assumptions:

(*a*) The smallest eddies which are smaller than the laminar flame front thickness penetrate the front to increase the internal diffusion process and thus the thickness of the flame; this process is repeated until equilibrium is reached between convective and diffusive effects, leading to a thickened flame front of thickness δ^*.

(*b*) Turbulent eddies which are larger than the effective flame front thickness δ^* wrinkle the front to increase the effective front surface; the increase in flame speed is proportional to the area increase due to the turbulence.

The application of this model to LES is straightforward. The turbulent large scales u_t and l_t only enter Zimont's analysis via the energy dissipation rate $\epsilon \sim u_t^3/l_t$, which holds for any length scale l and associated velocity scale u_l in the Kolmogorov cascade, $\epsilon \sim u_l^3/l$, where $l_t \geq l \geq \eta$. This implies that we can replace the turbulent large-scale fluctuations by the fluctuations at the cut-off scale (u_Δ, Δ), provided that the large-eddy filter scale Δ is larger than the flame thickness δ^*. We obtain for the turbulent flame speed S_t^Δ defined at the cutoff level,

$$\frac{S_t^\Delta}{S_l} = 1 + A\,(\mathrm{Re}_\Delta \mathrm{Pr})^{1/2}\,\mathrm{Da}_\Delta^{-1/4}, \tag{2.12}$$

where

$$\mathrm{Re}_\Delta = \frac{u_\Delta \Delta}{\nu}, \quad \mathrm{Da}_\Delta = \frac{\Delta}{u_\Delta \tau_c}. \tag{2.13}$$

The original formulation of Zimont (1979) has been modified to recover the laminar flame speed in regions of low turbulence activity. Equation (2.12) also includes a proportionality constant A of order unity. $A = 0.52$ was found by Zimont & Lipatnikov (1995), where turbulent flame speeds were computed from integral turbulent scales. Assuming that the subgrid closure results in the appropriate level of energy dissipation, the same model constant has been used in the present study.

The filter scale Δ is obtained from the box filter over grid cells

$$\Delta = 2(\Delta_x \Delta_y \Delta_z)^{1/3}, \tag{2.14}$$

and the subgrid scale velocity u_Δ is estimated from the Smagorinski subgrid viscosity as

$$u_\Delta = \frac{\nu_t}{C_s \Delta} = C_s \Delta \sqrt{2\overline{S}_{ij}\overline{S}_{ij}}. \tag{2.15}$$

It is to be noted that the model formulation is now grid dependent, and it should be verified that the flame thickness does not exceed the grid scales, i.e. $\mathrm{Da}_\Delta > 1$. Indeed, Zimont *et al.* (1997) estimate $\mathrm{Da} = 3$ for a gas turbine burner which would invalidate the subgrid closure if $\Delta \ll l_t$.

2.3. *The effect of flame stretch*

Equation (2.12) leads to larger flame speeds for increasing turbulence intensity; however, at very high levels of turbulence intensity, it is observed experimentally that the turbulent burning rate is limited or may even decrease (Zimont & Lipatnikov 1995). This "bending effect" has been incorporated in (2.12) by introducing a stretch parameter G as a correction factor for the turbulent burning velocity (Zimont & Lipatnikov 1995), which we adopt here at the velocity subgrid level. G is the probability of unquenched flamelets and is defined as

$$G = \frac{1}{2}\mathrm{erfc}\left\{-\left(\frac{1}{2\sigma}\right)^{1/2}\left[\ln\left(\frac{\epsilon_{cr}}{\epsilon}+\frac{\sigma}{2}\right)\right]\right\}. \tag{2.16}$$

$\sigma \simeq \ln(\Delta/\eta)$ is the standard deviation of the log-normal distribution of the dissipation rate $\epsilon = u_\Delta^3/\Delta$, and $\epsilon_{cr} = 15\nu g_{cr}^2$. g_{cr} is a critical flamelet quench rate that is obtained either from laminar flame computations or can be estimated from $g_{cr} \sim S_l^2/\chi$.

In writing (2.16) for the turbulent flame speed at the grid cut-off level, we assume that the significant contribution for the dissipation spectrum is contained entirely in the subgrid scales. For very low dissipation rates $\epsilon \ll \epsilon_{cr}$, no flame quenching occurs ($G = 1$). For very high dissipation rates $\epsilon \gg \epsilon_{cr}$, all flames are quenched locally by the turbulence ($G = 0$). It should be noted that the modeling of flame quench in this way is only qualitatively correct. In particular, estimates of the appropriate stretch rate g_{cr} are connected with relatively large uncertainties; for more details see Polifke *et al.* (2000). Also, (2.16) does not take into account unsteady effects which are known to be very important for extinction and (re-)ignition.

The uncertainty of this model parameter is perhaps mostly related to the fact that G depends on the entire turbulence spectrum. Specifically, G decreases for smaller Kolmogorov scales at constant ϵ, ϵ_{cr}. In fact, no clear experimental evidence exists for flame extinction by small-scale turbulence, let alone its dependence on Reynolds number. Indeed, the simulations by Meneveau & Poinsot (1991) suggest that the smallest eddies have no effect on the flame front mainly because their lifetime is too short. Further research is necessary to clarify whether (2.16) is appropriate in a LES context or whether the flame stretch should be associated only with the largest turbulent motions which are explicitly computed.

In this work, the application of the stretch parameter at the subgrid level was found to be crucial in the case of a flame that is stabilized in the vicinity of a backward-facing step (see Section 4), and a similar finding has been reported by Weller *et al.* (1998). Flamelet straining reduces the effective reaction rate close to the expansion, which has a large impact on the local heat release in the flame-front roll-up.

3. Numerical implementation

Equation (2.7) has been implemented in a standard industrial flow solver (Fluent 5). This solver provides a basic LES capability of cold flow simulations with the standard Smagorinski subgrid closure with near-wall damping and approximate log-law wall boundaries. The unstructured finite-volume solver uses second-order central differencing for convective momentum fluxes and second-order upwinding for scalar fluxes (such as for the reaction progress variable c). The SIMPLE pressure-correction scheme is used for time-advancement; discretization of pressure in the correction step is second-order accurate.

test case	grid ($N_x \times N_r \times N_\phi$)	resolution (r^+)
DNS_IFS	$38 \times 32 \times 64$	0.6
DNS_REF	$38 \times 32 \times 64$	0.6
DNS_FINE	$64 \times 32 \times 128$	0.3

TABLE 1. Setup for pipe flow at $\mathrm{Re}_\tau = \frac{u_\tau R}{\nu} = 180,\ R = 1,\ L = 10$.

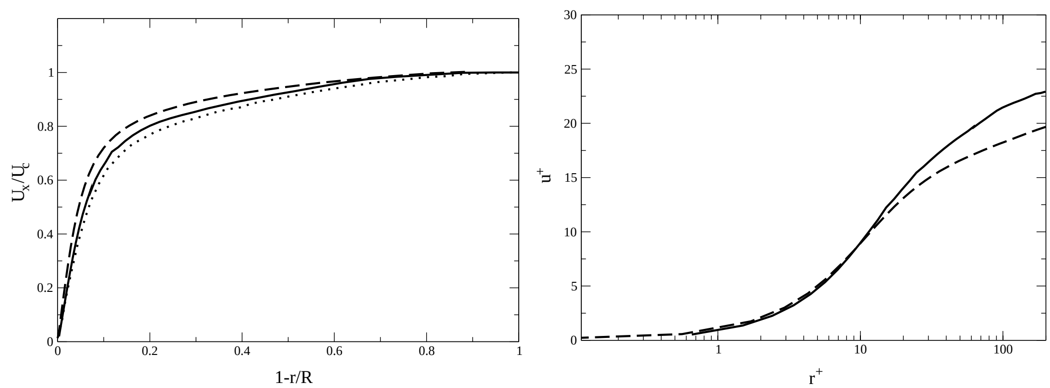

(a) (b)

FIGURE 1. Mean flow profiles. (a) velocity scaled with center line velocity U_c; (b) velocity scaled with friction velocity $u_\tau = \sqrt{\tau_w/\rho}$. Symbols: DNS_{IFS} (———); DNS_{REF} (– – – –); DNS_{FIN} (········).

This setup is generally acceptable for performing engineering-level LES. However, because no validation data exists for the LES implementation, it was felt that a basic solver validation should be carried out as part of this study. The capabilities of the flow solver to resolve the turbulent fluctuations were assessed at the most basic level: Is the solver capable of maintaining statistically steady turbulence in a periodic wall-bounded flow, or does the inherent numerical diffusion damp out all fluctuations? If turbulence can be maintained, how do statistics compare with those obtained from the thoroughly validated flow solver that has been developed at CTR?

To exclude any effects of the subgrid closure and the approximate wall model, a DNS of streamwise periodic pipe flow was chosen as a test case. The parameters of the setup and flow are given in table 1. The computation with Fluent (DNS_IFS) is compared with two results that were obtained with CTR's DNS code; DNS_REF is a reference computation on the same grid, and DNS_FINE is a reference computation at higher resolution. The reference flow solver is also second-order accurate.

The results for the mean flow profiles are presented in Fig. 1. While the rescaling with the center line velocity (Fig. 1a) suggests that the accuracy of DNS_IFS is in between the reference computations at different resolutions, the rescaling with the friction velocity in Fig. 1b reveals that the velocity levels in the log-law region are overestimated by at least 10%. This is an indication for stronger damping in the near-wall region for Fluent

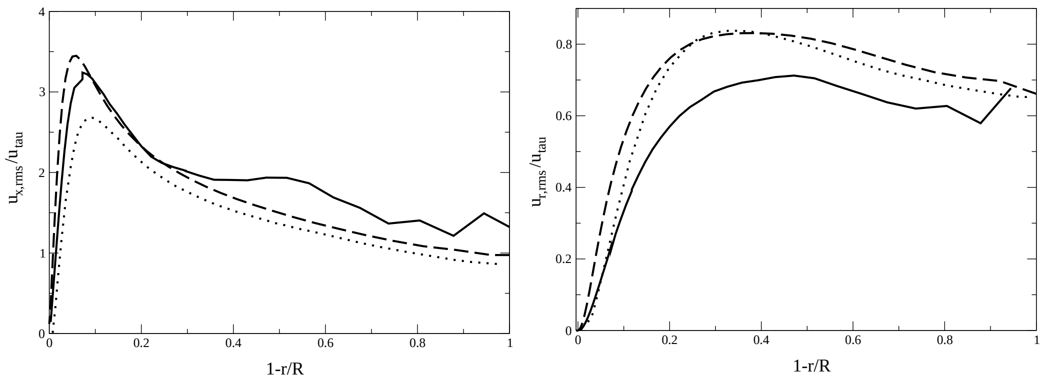

(a) (b)

FIGURE 2. Velocity fluctuations of the resolved scales, normalized with the friction velocity. (a) - streamwise fluctuations; (b) - radial fluctuations. See Fig. 1 for symbols.

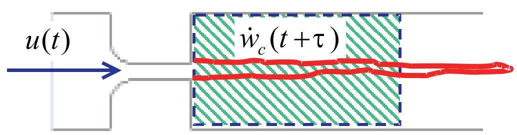

FIGURE 3. Sketch of the simple jet flame from the experiment by Poinsot *et al.* (1987).

which is likely to be due to higher levels of numerical diffusion. This is confirmed by the second-order statistics which are presented in Fig. 2. While streamwise fluctuations display a reasonable agreement with the reference computations, Fig. 2b reveals that wall-normal fluctuations are significantly underpredicted. It is also interesting to note that computing times for Fluent are about 100 times slower than for the optimized DNS flow solver (corresponding to several days on a 4-processor workstation for a full simulation). However, in light of the fact that the time-advancement scheme is not optimized for a simulation where the timestep is limited by the smallest turbulent time scale and usually not by numerical stability, and given that an unstructured general purpose code is compared here with a structured, vectorized solver, this overhead is, in fact, acceptable.

4. Application to a model combustor

The TFC subgrid closure model has been applied to a generic premixed propane-air jet flame that is stabilized in the expansion behind the injection slot; the configuration, shown in Fig. 3, is based on an experiment by Poinsot *et al.* (1987). The experiment consisted of five parallel, essentially two-dimensional slots, of which one is indicated in the sketch. The experiments showed various modes of instability with strong self-excited oscillations. The mode at 530Hz was found to be one of the most unstable.

The self-excitation of combustion instabilities is linked to the phase relationship between the acoustic pressure field and unsteady heat release via Rayleigh's criterion. The criterion implies that acoustic instabilities are amplified if pressure and heat release fluctuations are in phase. The phase relationship is thus important when quantifying the stability properties of a burner, and it is used here to qualify the usefulness of the LES flame speed closure for the simulation of unsteady combustion.

numerical setup				model parameters				
no. cells	Δ_{min}	u_{in}	Δt	S_l	T_u	T_{ad}	χ	g_{cr}
31500	0.1mm	6.4 m/s	$5 \cdot 10^{-6}$	0.36 m/s	300 K	2190 K	$2.2 \cdot 10^{-5}$	6000 1/s

Table 2. Setup for slot burner of a premixed, stoichiometric propane-air flame at atmospheric conditions.

4.1. *Setup and model parameters*

The numerical simulation is based on a single slot with symmetry conditions at the top and bottom boundaries as indicated in Fig. 3. We adopt here the model setup by Angelberger *et al.* (1998), who numerically investigated this combustor with a flame model based on artificial flame front thickening. The computations were performed in two dimensions since flow visualizations in the experiment have indicated that large-scale structures produced by the unsteady combustion were essentially two-dimensional, and the computations by Angelberger *et al.* (1998) have indicated that this assumption is reasonable.

Parameters of the setup and the combustion model parameters are summarized in table 2. The model parameters for the TFC model are based on the detailed chemistry calculations presented in Angelberger *et al.* (1998), while the critical strain parameter g_{cr} is based on the rescaling procedure proposed in Polifke *et al.* (2000) to estimate critical flame stretch in a fresh-to-burnt, opposed jet configuration. The local Damköhler number has been estimated for this configuration as $\mathrm{Da}_\Delta > 2$, and the assumption of combustion in the thickened flamelet regime with flame thickness below the subgrid level is expected to hold.

The numerical setup does not contain the feedback between heat release and acoustic fields because it is based on the incompressible (but variable density) flow equations. Therefore, the self-excited instability from the experiment is simulated via the artificial situation where the incoming mass flow rate is varied (assuming that the acoustic perturbations do not travel upstream to the fuel injector such that the fuel-air equivalence ratio could be altered). The amplitude of the mass flow variations was set to $\pm 25\%$ of the mean flow rate, which is comparable to the experimentally observed fluctuation levels, and the single-frequency, sinusoidal forcing was fixed at 530Hz, corresponding to the strongest instability mode in the experiment.

4.2. *Results*

The forced simulations were started after an initial transient in which the statistically steady flame was established, starting from steady-state computations. In Fig. 4 we plot snapshots of the unstable flame during one cycle of oscillation; as in the experiment, the formation of mushroom like vortices is observed in the simulation. However, the vortices form significantly further downstream than in the experiment as indicated in Fig. 4*(c)* where we compare directly with a snapshot of the experiment obtained at the same phase angle within the 530Hz cycle. A possible explanation for this effect is that the definition of u_Δ does not take into account dilatation effects, and thus the turbulent flame speed is likely to be overestimated in regions of relatively weak turbulence intensity where a

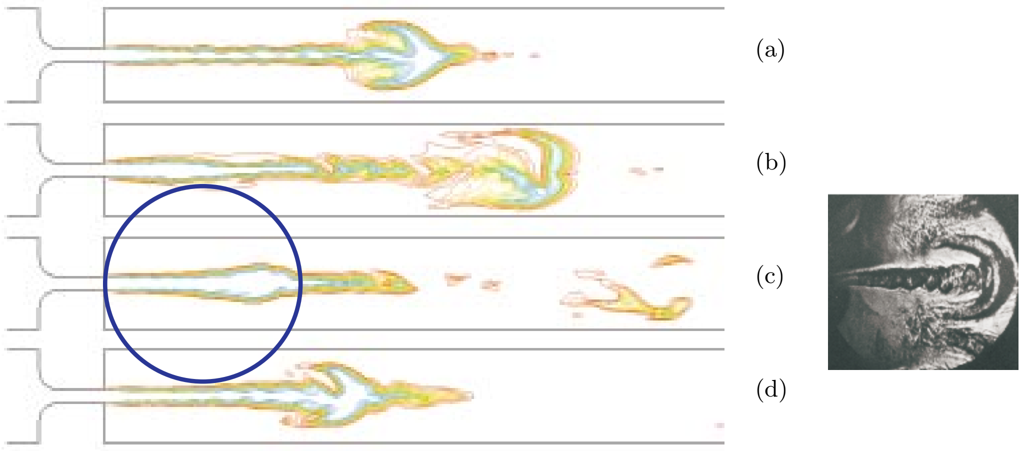

FIGURE 4. Instantaneous snapshots of the reaction progress variable during one forcing cycle at 530 Hz. The time between each picture corresponds to a quarter period. Also included in the figure is a snapshot taken from Poinsot *et al.* (1987), obtained at the same phase angle.

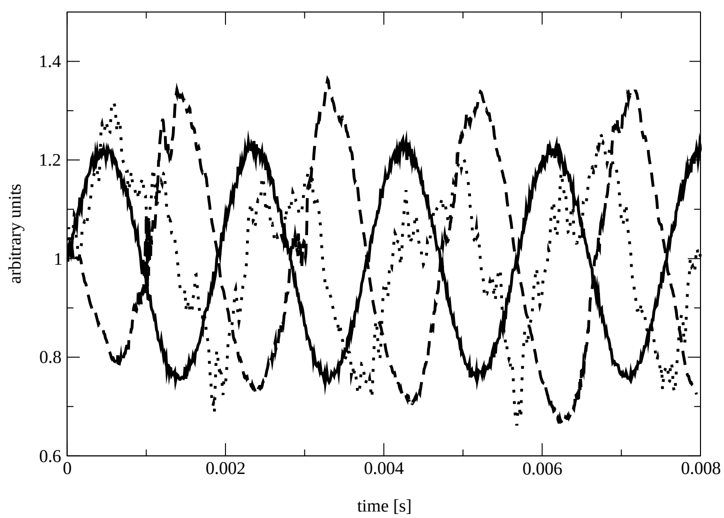

FIGURE 5. Time history of reaction rates with and without flame stretch. Symbols: ——— , inflow rate; - - - - , reaction rate; ········ , reaction rate, no stretch.

roll-up would otherwise be observed. More sophisticated approaches to model u_Δ are suggested in Colin *et al.* (2000).

Box-averaging the heat release rate over a region that resembles the observation window from the experiment (see Fig. 3) allows one to measure the phase-lag τ between reaction rate $\overline{w_c}(t+\tau)$ and forced inflow rate $\overline{u}(t)$; both numerical and experimental results are plotted in Fig. 5. Initially, numerical simulations were carried out with the correction factor $G = 1$ everywhere because the effects of flame quenching were considered negligible in a case where turbulence levels are generally moderate. However, without the stretch

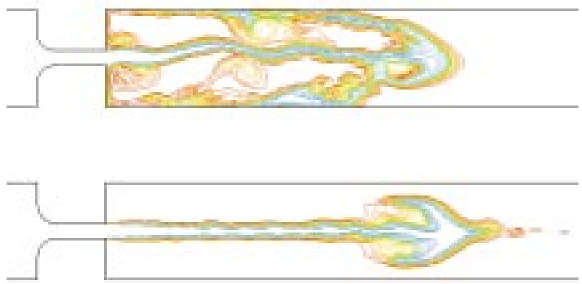

FIGURE 6. Snapshots of the ECB burner. Effect of flame stretch.

factor the heat release rate peaks immediately after the area expansion, and this peak remains attached throughout the forcing cycle, leading – contrary to the experiment where a phase angle of π has been measured – to an almost in-phase relation between heat release and inflow rate as also indicated in Fig. 5. This behavior is unphysical because the large strain in the vicinity of the step leads to reduced reaction rates and thus a detachment of the flame. Applying the stretch factor (2.16) to this configuration significantly altered the situation; the flame was detached and the phase-angle π from the experiment was recovered as shown in Fig. 5. A possible weakness of the model is the presence of the reaction rate reduction parameter in the entire flow field. One consequence of this is that the instantaneous flame structures are strongly affected by the extinction strain rate. In Fig. 6 we show two snap-shots at the same phase angle within the forcing cycle. While the lower figure is obtained with a stretch parameter $g_{cr} = 6000$, the upper figure corresponds to $g_{cr} = 2000$ (corresponding to the extinction strain for the opposed jet configuration of fresh mixtures). Obviously, local variations in reaction rates are observed; more importantly, however, the general flame shape, i.e. the formation of the vortices and their phase-angle, is found to be very insensitive to the absolute value of this model parameter, which is not known with great accuracy.

5. Conclusions

A model for premixed turbulent combustion based on a turbulent flame speed closure (TFC) has been proposed in the context of large-eddy simulations. The model is an extension of the original formulation in a RANS context. Possible limitations of the model due to its definition at the cutoff level and the uncertainties in modeling subgrid flame quenching have been broadly discussed.

The model has been applied to a simple premixed jet flame in a backward-facing step combustor. The results have indicated that a large-eddy simulation based on the TFC model is able to predict the forced combustor response. The agreement with a self-excited instability mode at the same frequency as observed in the experiment is good in terms of its phase angle between the incoming flow rate and the box-window integrated heat release rate.

The simulations in this study were based on a general-purpose industrial flow solver which includes basic LES capabilities but which has not yet been validated in detail. A simple validation study of a resolved low Reynolds number pipe flow revealed that the solver is capable of reproducing first and second-order statistics with reasonable accuracy. While further validation work is necessary for both the flow solver and the TFC-LES combustion model, the tool developed here appears to be appropriate to study a full-scale gas turbine combustor in the near future.

Acknowledgments

We gratefully acknowledge the help by G. Iaccarino and C. D. Pierce in supporting the code validation and performing the reference computations from Section 3.

REFERENCES

Angelberger, C., Veynante, D., Egolfopoulos, F., & Poinsot, T. 1998 Large eddy simulations of combustion instabilities in premixed flames. In *Proceedings of the Summer Program* (Center for Turbulence Research, NASA Ames/Stanford Univ.) 61-82.

Colin, O., Ducros, F., Veynante, D., & Poinsot, T. 2000 A thickened flame model for large eddy simulations of turbulent premixed combustion. *Phys. Fluids.* **12**, 7.

Kim, W.-W., Menon, S., & Mongia, H. C. 1998 Large-eddy simulation of a gas turbine combustor flow. *Comb. Sci. and Tech.* **143**, 25-62.

Meneveau, C., & Poinsot, T. 1991 Stretching and quenching of flamelets in premixed turbulent combustion. *Combustion and Flame.* **86**, 311-332.

Peters, N. 2000 *Turbulent combustion*, Cambridge University Press.

Poinsot, T., Trouve, A., Veynante, D., Candel, S., & Esposito, E. 1987 Vortex driven acoustically coupled combustion instabilities. *J. Fluid Mech.* **177**, 265-292.

Polifke, W., Flohr, P., & Brandt, M. 2000 Modeling of inhomogeneously premixed combustion with an extended TFC model. In *Proceedings of ASME TURBO EXPO 2000* 2000-GT-0135.

Veynante, D., & Poinsot, T. 1997 Reynolds-averaged and large eddy simulation modeling for turbulent combustion. In *New tools in turbulence modeling*, O. Metais & J. Ferziger Eds., Les Editions de Physique.

Weller, H. G., Tabor, G., Gosman, A. D., & Fureby, C. 1998 Application of a flame-wrinkling LES combustion model to a turbulent mixing layer. In *27th Int. Symp. on Combustion*, The Combustion Institute, 899-907.

Zimont, V. L. 1979 The theory of turbulent combustion at high Reynolds numbers. *Combust. Expl. and Shock Waves.* **15**, 305-311.

Zimont, V. L., Biagioli, F., & Syed, K. J. 2000 Modelling turbulent premixed combustion in the intermediate steady propagation regime. *Int. J. Comp. Fluid Dyn.* **1**(1-3).

Zimont, V. L., & Lipatnikov, A. N. 1995 A numerical model of premixed turbulent combustion of gases. *Chem. Phys. Reports.* **14**(7), 993-1025.

Zimont, V. L., Polifke, W., Bettelini, M., & Weisenstein, W. 1997 An efficient computational model for premixed turbulent combustion at high Reynolds numbers based on a turbulent flame speed closure. *J. Eng. for Gas Turb. and Power, Transactions of the ASME.* **120**, 526-532.